American Mineralogist, Volume 88, pages 1955–1969, 2003

The Composition and Morphology of Amphiboles from the Rainy Creek Complex, Near Libby, Montana

G.P. MEEKER,[1,*] A.M. BERN,[1] I.K. BROWNFIELD,[1] H.A. LOWERS,[1,2] S.J. SUTLEY,[1] T.M. HOEFEN,[1] AND J.S. VANCE[3]

[1]U.S. Geological Survey, Denver Microbeam Laboratory, Denver, Colorado 80225, U.S.A.
[2]Colorado School of Mines, Golden, Colorado, 80401, U.S.A.
[3]U.S. Environmental Protection Agency, Region 8, Denver, Colorado 80204, U.S.A.

ABSTRACT

Thirty samples of amphibole-rich rock from the largest mined vermiculite deposit in the world in the Rainy Creek alkaline-ultramafic complex near Libby, Montana, were collected and analyzed. The amphibole-rich rock is the suspected cause of an abnormally high number of asbestos-related diseases reported in the residents of Libby, and in former mine and mill workers. The amphibole-rich samples were analyzed to determine composition and morphology of both fibrous and non-fibrous amphiboles. Sampling was carried out across the accessible portions of the deposit to obtain as complete a representation of the distribution of amphibole types as possible. The range of amphibole compositions, determined from electron probe microanalysis and X-ray diffraction analysis, indicates the presence of winchite, richterite, tremolite, and magnesioriebeckite. The amphiboles from Vermiculite Mountain show nearly complete solid solution between these end-member compositions. Magnesio-arfvedsonite and edenite may also be present in low abundance. An evaluation of the textural characteristics of the amphiboles shows the material to include a complete range of morphologies from prismatic crystals to asbestiform fibers. The morphology of the majority of the material is intermediate between these two varieties. All of the amphiboles, with the possible exception of magnesioriebeckite, can occur in fibrous or asbestiform habit. The Vermiculite Mountain amphiboles, even when originally present as massive material, can produce abundant, extremely fine fibers by gentle abrasion or crushing.

INTRODUCTION

The Rainy Creek alkaline-ultramafic complex (Fig. 1) contains a world-class vermiculite deposit formed by hydrothermal alteration of a large pyroxenite intrusion. The deposit is located at Vermiculite Mountain (also called Zonolite Mountain) approximately six miles northeast of Libby, Montana. The mine began operations circa 1920 and closed in 1990. Recent attention has been given to fibrous and asbestiform amphiboles associated with vermiculite ore produced at Vermiculite Mountain. The amphiboles are suspected to be a causative factor in an abnormally high number of cases of respiratory diseases in the residents of Libby and the former mine and mill workers (Lybarger et al. 2001).

The presence of fibrous and asbestiform amphiboles in the vermiculite and mine waste from Vermiculite Mountain has triggered a Superfund action that ranks among the largest and most costly in the history of the U.S. Environmental Protection Agency. The ultimate resolution of the problems associated with contamination by these materials will be years in coming, and the final costs in both human health and dollars may be enormous. These issues necessitate a very thorough understanding of the morphological and chemical properties of the amphiboles associated with the Vermiculite Mountain deposit. It is these properties that are of ongoing concern with respect to future regulatory policies and investigations into possible mechanisms of toxicity of fibrous and asbestiform amphiboles (Ross 1981; Langer et al. 1991; Kamp et al. 1992; van Oss et al. 1999).

Previous studies of the composition and morphology of the amphiboles from Vermiculite Mountain are limited in number. Wylie and Verkouteren (2000) studied two amphibole samples from the vermiculite mine. They determined the amphibole in both samples to be winchite based in part on chemistry, using the classification system of Leake et al. (1997), and on optical properties. Gunter et al. (2003) confirmed the findings of Wylie and Verkouteren (2000) on the same two samples and analyzed three additional ones, which they also determined to be winchite based on optical microscopy, electron probe microanalysis, and Mössbauer spectroscopy. Indeed, the results of the present study demonstrate convincingly that the vast majority of the amphiboles from Vermiculite Mountain are winchite as currently defined by the International Mineralogical Association (Leake et al. 1997). Previously, the amphibole from Vermiculite Mountain had been called soda tremolite (Larsen 1942), richterite (Deer et al. 1963), soda-rich tremolite (Boettcher 1966b), and tremolite asbestos and richterite asbestos (Langer et al. 1991; Nolan et al. 1991).

* E-mail: gmeeker@usgs.gov

0003-004X/03/1112–1955$05.00

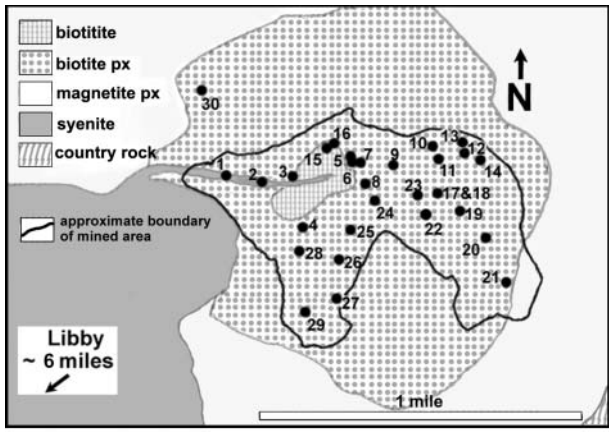

FIGURE 1. Map of vermiculite mine showing amphibole sampling locations. Geology after Boettcher (1967). The geology, as depicted here, may not completely coincide with the present-day surface geology because of the mining activity between 1967 and 1992. Therefore, the sampling points may not coincide in all cases with the rock units as shown above.

The chemical and physical properties of the fibrous amphiboles from Vermiculite Mountain are of significance for two reasons. The first is that most asbestos regulations specifically cite five amphibole asbestos "minerals:" tremolite, actinolite, anthophyllite, amosite, and crocidolite; and one serpentine mineral, chrysotile. These names have evolved from a combination of mineralogical and industrial terminology. The mineral names richterite and winchite do not appear in existing regulatory language. It is therefore important to understand fully the range of amphibole compositions present so that appropriate terminology can be applied to this material. The second, and perhaps more important reason, is that the mechanisms for the initiation of asbestos-related diseases are not fully understood. If the fibrous and asbestiform amphiboles from Vermiculite Mountain are truly a different type of amphibole than has been studied previously by the medical community, then it is important to understand and describe the full range of chemical and physical properties of this material for future toxicological and epidemiological studies.

The current study was designed to provide a systematic evaluation of the Vermiculite Mountain amphiboles and to specifically answer four important questions: (1) are the amphiboles from Vermiculite Mountain relatively uniform in composition or is there a broad range of compositions; (2) what morphologic characteristics are present within the population of Vermiculite Mountain amphiboles; (3) are there any correlations among chemistry, mineralogy, and morphology; and (4) what are the chemical and physical characteristics of the fibrous and asbestiform amphiboles that are of respirable size? The answers to these questions are of importance to the members of the asbestos community who are involved with developing regulatory language, studying the health effects of asbestos, and planning responsible mining and processing activities. The present study provides a framework with which to evaluate the range of compositions and morphologies of the Vermiculite Mountain amphiboles in the context of existing industrial, medical, regulatory, and mineralogical definitions.

GEOLOGIC BACKGROUND

The Rainy Creek complex (Fig. 1) has been described as the upper portion of a hydrothermally altered alkalic igneous complex composed primarily of magnetite pyroxenite, biotite pyroxenite, and biotitite (Pardee and Larsen 1928; Bassett 1959; Boettcher 1966a, 1966b, 1967). The original ultramafic body is an intrusion into the Precambrian Belt Series of northwestern Montana (Boettcher 1966b). A syenite body lies southwest of and adjacent to the altered pyroxenite and is associated with numerous syenite dikes that cut the pyroxenites. A small fenite body has been identified to the north, suggesting the presence of a carbonatite at depth (Boettcher 1967). The amount of vermiculite within the deposit varies considerably. At different locations, the vermiculite content of the ore ranges from 30 to 84% (Pardee and Larsen 1928). Subsequent alkaline pegmatite, alkaline granite, and quartz-rich veins cut the pyroxenites, syenite, and adjacent country rock. It is in the veins and wall rock adjacent to these dikes and veins that a significant portion of the fibrous amphiboles occur as a result of hydrothermal processes (Boettcher 1966b). The dikes, veins, and associated wall-rock alteration zones range in width from a few millimeters to meters, and are found throughout the deposit. Fibrous and massive amphiboles are the most abundant alteration and vein-filling products. Estimates of the amphibole content in the alteration zones of the deposit range from 50 to 75% (Pardee and Larsen 1928). Accessory alteration minerals include calcite, K-feldspar, talc, vermiculite, titanite, pyrite, limonite (formed by pyrite oxidation), albite, and quartz. In addition, "primary" pyroxene, biotite, and hydrobiotite are present in varying amounts.

METHODS

Sample collection

Sampling of the amphibole from Vermiculite Mountain was done in the spring of 2000 with the purpose of collecting a representative suite of amphibole compositions contained within the mined area of the vermiculite deposit. Samples were collected based on a grid designed to provide statistically significant sampling over the accessible areas of the mine. Due to the nature of both the geology of the deposit and the physical conditions in the mine resulting from past reclamation efforts, samples could only be collected from nearly vertical "cut faces" in the mine. We therefore sampled from the closest vertical cut face to each grid node.

A total of 30 locations from the mine area were sampled (Fig. 1). On average, samples were approximately 1–2 kilograms in weight. Samples were selected to provide the maximum variability from location to location in an attempt to fully characterize the range of amphibole compositions and textures present in the deposit. Samples from some locations displayed a massive texture, whereas more friable materials occurred in other locations. In some locations, veins were only a few centimeters in width. At other sampling points, the veins of amphibole-rich rock were as wide as four meters. In these cases, an attempt was made to sample from the edge of the exposed vein as well as the center to look at compositional changes across the vein. In a few cases, veins and adjacent rock appeared to be nearly pure amphibole.

Sample preparation

All of the samples, whether fibrous and friable or massive, produced extremely fine fibrous dust when broken or abraded. The presence of this dust necessitated that all sample preparation steps, including preparation of polished

thin sections, be carried out in a negative-pressure, stainless steel, HEPA-filtered hood. Each sample was examined, as collected, in the hood, and representative pieces were selected for X-ray diffraction (XRD), electron probe microanalysis (EPMA) using wavelength dispersive spectroscopy (WDS), and scanning electron microscopy combined with energy dispersive X-ray analysis (SEM/EDS). For each sample location, an effort was made to find pieces that appeared to be representative of the total sample. Samples selected for EPMA were prepared as polished petrographic thin sections, and detailed optical micrographs were made for later reference. In addition, one or more SEM stubs were prepared for each sample by touching a sample stub covered with a disk of conductive C tape to the inside of each plastic sample bag. This method allowed us to collect and analyze the friable and fibrous components of each sample so that these portions could be distinguished from the non-friable material. The distribution of amphibole types within the friable material could thus be determined. A portion of a typical SEM mount is shown in Figure 2.

Sample analysis

In the present study, we used a combination of three analytical techniques to characterize composition, mineralogy, and morphology of both the fibrous and non-fibrous components of the Vermiculite Mountain amphiboles. None of these analytical techniques alone is capable of accomplishing this task. XRD was used to determine and confirm the presence of amphibole by structural analysis. EPMA/WDS of polished thin-sections was used to derive accurate compositions of the amphiboles present, and SEM/EDS was used to characterize the morphology and to determine the amphibole mineral distribution among individual small fibers that are of respirable size and are generally too small to mount and polish. The SEM-based EDS analysis of small, unpolished fibers does not have the accuracy to definitively identify the amphibole types present. However, when combined and correlated with EPMA/WDS analysis for each individual sample the SEM/EDS analyses show the distributions of the fibrous and asbestiform minerals present in the deposit.

X-ray diffraction analysis

Splits of each sample were analyzed by XRD at the USGS analytical laboratories in Denver. Two grams of material were prepared by hand grinding the sample in an agate mortar and pestle and then wet micronizing (to decrease lattice shear) in a micronizing mill to obtain an average grain size of 5 micrometers. This procedure was used to minimize the orientation effects of the minerals present. The samples were air dried and packed into an aluminum holder for subsequent mineralogical analysis. The powder XRD data were collected using a Philips APD 3720 automated X-ray diffractometer with spinning sample chamber, a diffracted beam monochromator, and Ni-filtered Cu$K\alpha$ radiation at 40 kV and 25 mA. The data were collected at room temperature in scanning mode, with a step of 0.02 °2θ and counting time of 1 second at each step. The collected data were evaluated and minerals were identified using JADE+ software from Materials Data Inc.[1]

Qualitative mineralogy was determined for each sample as major (>25% by weight), minor (5–25%), and trace (<5%). Our detection limit for these analyses was approximately 1–2 wt%. Table 1 shows samples ranging from fairly pure amphibole (samples 25, 28, and 30) to complex mixtures of many minerals (samples 7, 11, and 16). The primary amphibole minerals identified in each sample by matching reference X-ray data (JADE+) were winchite and richterite. Other minerals identified as major in some samples included calcite, talc, and dolomite. Minerals present at the minor level in many of the samples include calcite, K-feldspar, pyroxene, hydrobiotite, talc, quartz, vermiculite, and biotite.

The arrangement of the amphiboles into subgroups and series based on crystal-chemical considerations (Leake et al. 1997) is to a large extent a matter of convenience; considerable solid solution exists between one series and another, and even between one subgroup and another. Therefore, it is imperative that the final assignment of a specific amphibole name be based on a high-quality chemical analysis of the sample.

[1]The use of commercial product names in this manuscript is for information only and does not imply endorsement by the United States Government.

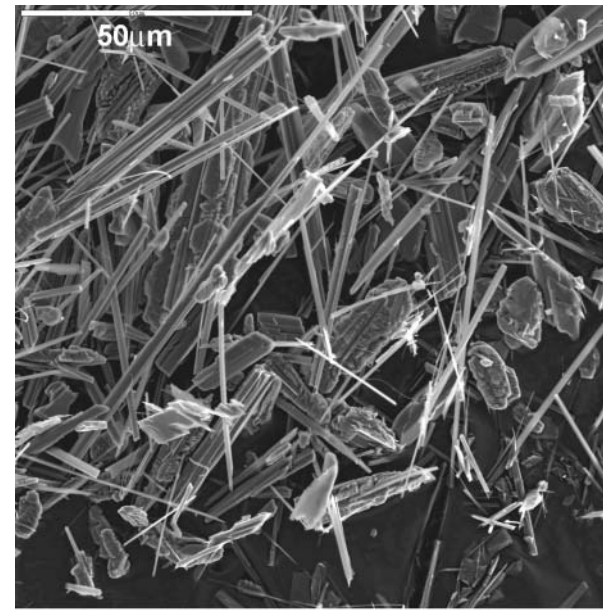

FIGURE 2. Area of the surface of a typical SEM sample stub prepared by touching the stub to the inside of the plastic sample bag. Most of the particles in the image are amphibole. Particle morphologies include acicular structures with high to low aspect ratios, bundles, and prismatic crystals. A few curved fibers can be seen in the image. Scale bar is 50 µm.

TABLE 1. Qualitative mineralogy by XRD

SAMPLE	MAJOR	MINOR	TRACE
1	rht/wht, tlc		qtz, kfs, vrm
2	rht/wht	cal	qtz, kfs,dol
3	rht/wht,cal	kfs	bt
4	rht/wht	tlc, aug, hbt	cal, dol
5	rht/wht	cal, kfs	hbt
6	rht/wht, cal		qtz, kfs
7	rht/wht	cal, aug	bt, vrm, kfs
8	rht/wht	cal	tlc, vrm, kfs, bt
9	rht/wht	cal	vrm, dol
10	rht/wht	cal, vrm	
11	rht/wht	cal, aug, kfs, tlc	qtz, vrm
12	rht/wht	kfs	
13	rht/wht	cal, tlc, di, kfs	
14	rht/wht	bt, kfs	cal, dol
15	rht/wht	cal, tlc	kfs
16	rht/wht	cal, aug, tlc, vrm	qtz, kfs
17	rht/wht	kfs, cal	bt
18	rht/wht	cal, kfs	bt
19	rht/wht	cal, kfs, aug	bt
20	rht/wht	cal	vrm
21	rht/wht	cal, tlc, hbt	kfs
22	rht/wht	cal, hbt, kfs	tlc
23	rht/wht	cal, kfs	
24	rht/wht	cal, kfs	
25	rht/wht		kfs, cal
26	rht/wht	cal, kfs, vrm	tlc, dol
27	rht/wht, cal		kfs
28	rht/wht		vrm, hbt
29	rht/wht, cal, dol		kfs
30	rht/wht	kfs	

Notes: Estimated concentration reported as major (>25 wt%), minor (>5%, <25%), and trace (<5%). Amphibole identification was determined by pattern structure using a best fit algorithm. Positive identification of amphiboles must rely on chemistry (see text). Mineral abbreviations used: rht/wht = richterite/winchite, tlc = talc, qtz = quartz, cal = calcite, kfs = potassium feldspar, vrm = vermiculite, dol = dolomite, bt = biotite, aug = augite, hbt = hydrobiotite, di = diopside.

Scanning electron microscopy and energy dispersive X-ray analysis

Images were obtained of representative areas of each sample stub (Fig. 2). Thirty or more fibers were analyzed in each of the 30 samples. Isolated fibers with diameters of 3 μm and less, representing the respirable fraction, were selected for analysis so as to minimize contributions of stray X-ray counts from nearby phases both laterally and vertically. One or more of the analyses from each sample set were discarded after later determination that the analysis contained unacceptable cation ratios, possibly due to contributions from adhering or nearby particles.

Scanning electron microscopy was performed using a JEOL 5800LV instrument, at the US Geographical Survey in Denver, operating in high-vacuum mode. Energy dispersive X-ray analysis was performed using an Oxford ISIS EDS system equipped with an ultra-thin-window detector. Analytical conditions were: 15 kV accelerating voltage, 0.5–3 nA beam current (cup), and approximately 30% detector dead time. All SEM samples were C coated. Data reduction was performed using the Oxford ISIS standardless analysis package using the ZAF option. Analyses were normalized to 100%. The quality of each EDS analysis was based on cation ratios and correlation with EPMA/WDS data (see below).

The matrix corrections used in these EDS analyses do not account for particle geometry. It is well known that such errors can be significant. However, Small and Armstrong (2000) have shown that, at 10–15 kV accelerating voltage, geometry-induced errors on particles can be relatively small. Our errors, in relative weight percent, estimated from analysis of 0.5–10 μm diameter particles of USGS, BIR1-G basalt glass reference material (Meeker et al. 1998) are approximately ±13% (1σ) for Na_2O, 4% for MgO and CaO, 3% for Al_2O_3, 2% for SiO_2, and 7% for FeO.

In addition to chemical EDS data on amphiboles from each sample stub, samples 4, 10, 16, 20, and 30 were selected for morphologic analysis of the amphibole particles. These samples were chosen to provide a representative range of compositions and textures. Size measurements were made using the Oxford ISIS software calibrated with a certified reference grid. For each sample, every amphibole (identified by EDS) was measured within a randomly chosen, 100×100 μm area of the stub. The minimum total number of particles counted was 300 per sample. One sample contained fewer than 300 amphiboles in one field of view, so a second field, not overlapping the first, approximately 25×25 μm in size was used to complete the data collection, using the same method as above. The maximum length and average width of each amphibole contained within or crossing into the field of view was used to calculate the aspect ratio (length/width) of each amphibole particle.

Wavelength-dispersive electron probe microanalysis

Electron microprobe analysis was performed on polished thin sections of 14 samples. The samples were selected based on their textural characteristics, mineralogy as determined by XRD and SEM/EDS, optical properties, and how representative the samples appeared to be of the entire suite. An attempt was made to include the full range of chemistries and textures.

Quantitative EPMA of the samples was performed using a five-wavelength spectrometer (WDS), fully automated, JEOL 8900 scanning electron microprobe, at the USGS in Denver. Analyses were obtained from areas that appeared to be representative of each sample by optical microscopy. Analytical conditions were: 15 kV accelerating voltage, 20 nA beam current (cup), point beam mode, and 20 second peak and 10 second background counting time. Calibration was performed using well-characterized silicate and oxide standards. Analytical precision for major and minor elements based on replicate analysis of standards was better than ±2% relative concentration for major and minor elements and equal to counting statistics for trace (<1 wt%) elements. Matrix corrections were performed with the JEOL 8900 ZAF software.

The friable nature of most of the samples caused some areas of the thin sections to exhibit plucking or poor polishing. Analyses within these areas commonly resulted in lower totals than would normally be acceptable on a polished surface. We rejected any EPMA analysis with an oxide total lower than 92 wt% (calculated H_2O in the Vermiculite Mountain amphiboles ranges from 1.72–2.11 wt%). The quality of the remaining analyses were judged by cation ratios. Analyses with unacceptable cation ratios (see below) were not included in the data reduction.

DATA ANALYSIS

The amphibole classification system of Leake et al. (1997) is based on site assignments for each cation in the structure. An accurate amphibole classification based on chemical analysis requires determination of the OH, ultra-light elements ($Z < 8$), and halogen content, as well as the oxidation state of Fe. Our EPMA analyses of the thin sections included F and Cl. It is not possible to analyze for OH, nor is it possible to accurately determine the ultra-light element content, particularly Li, by EPMA. It is unlikely, however, that Li is present in significant amounts because wet-chemical analyses of Vermiculite Mountain amphibole by previous investigators did not indicate Li (Deer et al. 1963). Also, USGS trace-element analyses of the 30 samples by ICRMS revealed Li (and other possible elemental constituents) at levels too low to be significant in cation calculations (P. J. Lamothe, personal communication). Finally, the stoichiometry that was evident upon data reduction of the EPMA data indicates that no significant components are missing from the analyses. The hydroxyl ion $(OH)^-$ was accounted for by the method described in Leake et al. (1997) by assuming a total anion charge of –2 for F + Cl + (OH).

Analyses were judged primarily on cation ratios for data corrected to 23 O atoms. Cations were assigned to crystallographic sites based on the methods outlined in Leake et al. (1997). In particular, all Si was assigned to the tetrahedral or T-site, followed by Al and then Ti, until the tetrahedral cation total equaled 8.00. Remaining Al and Ti, followed by Fe^{3+}, Mg, Fe^{2+}, and Mn, in that order, were assigned to the octahedral C-sites (M1, M2, and M3) until the C-site total equaled 5, or slightly less in some cases. Any remaining C-site cations, followed by Ca and Na, were assigned to the B-site (M4) until the site total equaled 2. All K and any remaining Na were assigned to the A-site. Because the Vermiculite Mountain amphiboles only include sodic, sodic-calcic, and calcic amphiboles as defined by Leake et al. (1997), it is primarily the distribution and cation totals of Ca, Na, and K in the B- and A-sites, and $Mg/(Mg + Fe^{2+})$ that determine the amphibole species.

A complete and correct application of the Leake et al. (1997) classification method requires knowledge of the oxidation state of Fe. Gunter et al. (2003), have determined Fe^{3+}/Fe^{total} in five samples of Vermiculite Mountain amphiboles to range from 0.56 to 0.76 using Mössbauer spectroscopy. Because of the large range of compositions of the amphiboles, we compared the results of calculating total Fe as Fe^{2+} vs. total Fe as Fe^{3+}. The difference in the handling of Fe made a small but significant difference in the distribution of the calculated amphibole species. Many analyses showed a change in mineral classification, as seen in Figure 3. The calculated stoichiometry of all EPMA analyses improved when total Fe was calculated as Fe^{3+}. In particular, the average number of Si cations based on 23 O atoms (anion charge = 46.0) decreased from 8.08 ± 0.07 with total Fe calculated as Fe^{2+} to 7.96 ± 0.06 with total Fe calculated as Fe^{3+}. Because the maximum Si content of the T-site in amphibole must be less than or equal to 8, within analytical error, these results suggest $Fe^{3+} > Fe^{2+}$, in agree-

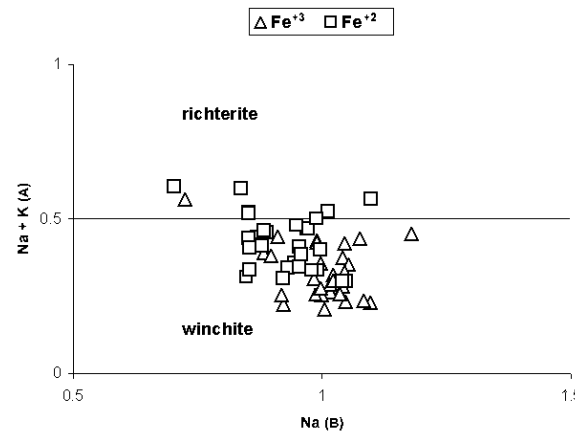

FIGURE 3. EPMA data from sample 14 plotted with all Fe calculated as Fe^{2+} and the same analyses plotted with all Fe calculated as Fe^{3+}. The **Y**-axis represents the amount of Na + K in the A-site of the amphibole structure, and the **X**-axis the amount of Na in the B-site. The boundary between winchite and richterite, as defined by Leake et al. (1997), is shown as a horizontal line at $^{A}(Na+K) = 0.5$. Note the approximate 25% decrease in the number of points plotting in the richterite field when all Fe is calculated as Fe^{+3}.

ment with the results of Gunter et al. (2003). To arrive at a better estimation of Fe^{3+}/Fe^{total} for each amphibole mineral, we chose 169 of the best EPMA analyses, representing a full range of compositions, and calculated Fe^{3+}/Fe^{total} for each individual analysis. The value for Fe^{3+}/Fe^{total} was determined by minimizing the deviation from ideal stoichiometry as described in Leake et al. (1997).

The average Fe^{3+}/Fe^{total} calculated from the best 169 EPMA analyses was 0.60, compatible with the values determined by Gunter et al. (2003). This average value was used to calculate the mineral distributions for the EDS analyses. This number will be least accurate for compositions close to tremolite and magnesioriebeckite (see below). However, the error introduced by using $Fe^{3+}/Fe^{total} = 0.60$ for all EDS analyses is significantly less than the analytical error for most of the major elements determined by EDS.

Amphibole classification derived from EDS results was also based on Leake et al. (1997). In general, the EDS data were very similar to the quantitative WDS results from EPMA. It was found, however, that the C-site totals from the EDS data averaged 3% below the ideal 5 cations. This deficiency could be due to the less-accurate standardless quantification routine, the fact that the analyses were performed on individual thin fibers rather than a polished surface or, more likely, a combination of both. In the Vermiculite Mountain amphibole, the primary cations in the C-site are Mg and Fe. In the cation site calculations, upon filling the C-site, any remaining C-site cations would be placed into the B-site. Increased residual C-site cations in the B-site would decrease the amount of Na in the B-site and increase the amount of Na in the A-site, thereby affecting the cation distributions and possibly the amphibole species classification. However, in our calculations using the more accurate EPMA/WDS data, residual C-site cations in the B-site were generally low or not present. Therefore, low totals in the C-site in the EDS data for these amphiboles should not cause significant errors in amphibole classification.

We attribute our low C-site totals in the EDS data to particle geometry and associated matrix correction errors primarily affecting Fe and possibly Mg, and not to actual differences between the friable and non-friable minerals in the Vermiculite Mountain amphibole. Based on our estimated analytical error for Fe and Mg, derived from the analysis of basalt glass particles (see above), and on the overall quality of each EDS analysis, we chose to incorporate EDS data points in which the C-site totals were 4.7 or higher or within 94% of the ideal 5 cations. With this error, the calculated compositions and site assignments on individual EDS analyses did not appear to change significantly or affect the mineral classification relative to the WDS data. A check on the validity of this argument can be seen in the sample-by-sample correlation of compositional distributions showing good agreement between EPMA/WDS and SEM/EDS data (Fig. 4). It is interesting to note that if the error in the C-site totals in the EDS data had been high rather than low, the distribution of amphibole species in the friable materials would likely have been skewed. An error of this type would be difficult to detect without EPMA/WDS data for comparison.

RESULTS

Chemistry

In general, the WDS (from EPMA) and the EDS data agree with respect to the amphibole species represented in each sample (Fig. 4). For some samples, the EPMA data show a narrower compositional range than the EDS data. This result is reasonable because EPMA analyses were performed on a single polished thin section for each sample, which may not represent the entire range of compositions of friable material found in a sample.

The data indicate that most of the Vermiculite Mountain amphiboles can be classified as one of three types, although it is possible that as many as six different amphiboles may be present, based on the Leake et al. (1997) classification criteria. Those minerals, in order of decreasing abundance, are: winchite, richterite, tremolite, and possibly magnesioriebeckite, edenite (see below), and magnesio-arfvedsonite. Representative EPMA analyses of the amphibole minerals are given in Table 2. For the respirable fraction, as determined by SEM/EDS, approximately 84% of the amphiboles can be classified as winchite, 11% as richterite, and 6% as tremolite.

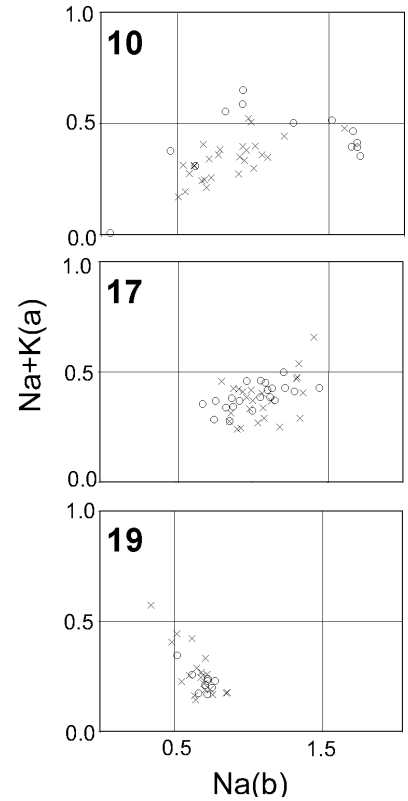

FIGURE 4. Cation values for Na in the B-site and Na + K in the A-site from individual samples show typical correlation between SEM (crosses) and EPMA (circles) data. Sample numbers are in the upper left corner of each plot.

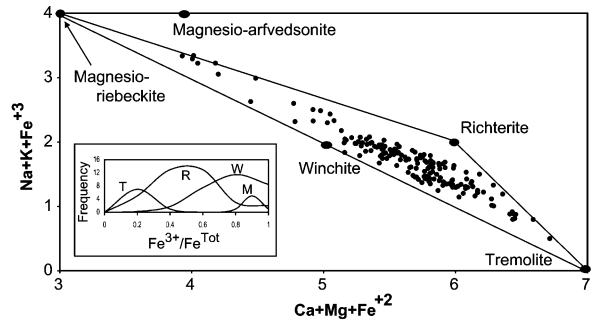

FIGURE 5. Amphibole compositions from the best 169 EPMA analyses, as determined from cation ratios, based on the criteria of Leake et al. (1997). End-member points for tremolite, winchite, richterite, magnesioriebeckite, and magnesio-afrvedsonite are shown. The data suggest that complete solid-solution may exist within the region defined by the tremolite, winchite, richterite, and magnesioriebeckite. Also shown (inset) are "best-fit" curves for the same data, showing calculated Fe^{+3}/Fe^{total} (see text) values for individual minerals where T=tremolite, R=richterite, W=winchite (multiplied by 0.25), and M=magnesioriebeckite.

Figure 5 shows the distribution of amphibole compositions found at the mine site at Vermiculite Mountain. The amphiboles range from nearly pure tremolite to compositions

TABLE 2. Representative wavelength dispersive of amphibole minerals

Sample	12	12	14	16	17	24	24	25	10	16	16
Mineral	W	W	W	W	W	W	W	W	T	T	T
Wt% Oxides											
F	0.21	0.27	0.18	0.20	0.58	0.31	0.52	0.43	0.21	0.17	0.20
Na_2O	3.39	4.45	4.21	3.29	3.54	3.13	4.47	2.70	2.61	2.26	2.27
MgO	22.3	19.2	20.5	21.4	19.8	21.3	20.9	21.7	22.0	23.0	22.0
Al_2O_3	0.15	0.17	0.16	0.46	0.37	0.15	0.33	0.11	0.16	0.60	0.52
SiO_2	58.7	57.1	57.2	57.7	56.8	57.5	57.7	57.5	57.1	56.4	56.6
Cl	BDL	BDL	BDL	BDL	BDL	BDL	BDL	BDL	BDL	BDL	BDL
K_2O	0.65	0.71	1.03	1.02	0.94	0.93	1.10	0.62	0.71	0.87	0.78
CaO	7.50	5.18	6.28	9.41	7.51	8.43	6.62	9.89	10.2	10.1	10.3
TiO_2	0.14	0.14	0.13	0.07	0.17	0.04	0.23	0.07	0.12	0.10	0.09
MnO	0.10	0.05	0.06	0.14	0.14	0.13	0.08	0.10	0.09	0.08	0.08
FeO-T	5.71	8.38	6.35	4.38	6.54	4.95	5.54	4.22	3.08	2.48	2.47
O ≡ F,Cl	0.09	0.11	0.07	0.08	0.24	0.13	0.22	0.18	0.09	0.07	0.08
□TOTAL	98.79	95.54	96.00	97.99	96.21	96.73	97.21	97.12	96.19	95.92	95.19
Structural Formula											
Si	7.988	8.000	7.990	7.987	7.993	7.988	7.987	7.994	7.997	7.904	7.986
Al^{iv}	0.012	0.000	0.010	0.013	0.007	0.012	0.013	0.006	0.003	0.096	0.014
Sum T-site	8.000	8.000	8.000	8.000	8.000	8.000	8.000	8.000	8.000	8.000	8.000
Al^{iv}	0.012	0.029	0.016	0.062	0.054	0.012	0.040	0.011	0.023	0.004	0.073
Ti	0.015	0.015	0.014	0.008	0.018	0.004	0.024	0.007	0.012	0.010	0.010
Fe^{vi}	0.340	0.981	0.682	0.052	0.498	0.415	0.524	0.178	0.038	0.024	0.036
Mg	4.531	3.976	4.264	4.423	4.153	4.421	4.306	4.489	4.599	4.813	4.627
Fe^{2+}	0.103	0.000	0.024	0.455	0.271	0.147	0.106	0.313	0.323	0.149	0.254
Mn	0.000	0.000	0.000	0.001	0.005	0.000	0.000	0.001	0.006	0.000	0.000
Sum C-site	5.000	5.000	5.000	5.000	5.000	5.000	5.000	5.000	5.000	5.000	5.000
Mg	0.000	0.031	0.000	0.000	0.000	0.000	0.000	0.000	0.000	0.000	0.000
Fe^{2+}	0.207	0.000	0.035	0.000	0.000	0.013	0.011	0.000	0.000	0.118	0.001
Mn	0.011	0.006	0.007	0.015	0.012	0.015	0.009	0.010	0.005	0.010	0.009
Ca	1.093	0.777	0.939	1.396	1.131	1.256	0.982	1.473	1.536	1.511	1.552
Na	0.688	1.187	1.018	0.589	0.858	0.716	0.998	0.517	0.459	0.362	0.438
Sum B-site	2.000	2.000	2.000	2.000	2.000	2.000	2.000	2.000	2.000	2.000	2.000
Na	0.207	0.021	0.121	0.293	0.109	0.127	0.203	0.210	0.249	0.253	0.183
K	0.112	0.128	0.183	0.179	0.168	0.165	0.195	0.109	0.128	0.156	0.140
Sum A-site	0.319	0.148	0.303	0.473	0.276	0.293	0.398	0.320	0.377	0.409	0.323
Total Cations	15.319	15.148	15.303	15.473	15.276	15.293	15.398	15.320	15.377	15.409	15.323

Notes: W = winchite, R = richterite, T = tremolite, MR = magnesioriebeckite, MA = magnesio-arfvedsonite, BDL = below detectability limit. Ferric Fe determined by stoichiometry.

continued

approaching end-member magnesioriebeckite. The majority of the compositions lie within the ternary field temolite-winchite-richterite, and all compositions lie within the field tremolite-richterite-magnesioriebeckite. The distribution of compositions suggests that complete solid solution exists within the compositional field shown. These results are compatible with the study by Melzer et al. (2000), who found evidence for complete solid solution in the experimental system K-richterite-richterite-tremolite.

Figure 5 also shows the distributions of Fe^{3+}/Fe^{total} for each amphibole species. These distributions suggest that Fe^{3+} is partitioned into each amphibole mineral according to crystal-chemical requirements. The complexities of such substitutions and the difficulties in identifying a specific substitution mechanism in amphiboles were discussed by Popp and Bryndzia (1992).

Actinolite was not found in our analyses of the Vermiculite Mountain amphiboles. Wylie and Verkouteren (2000) speculated on the presence of actinolite but were not able to make a determination in their samples because they did not calculate or otherwise determine the Fe^{3+} content. If our EPMA analyses were calculated with all Fe as Fe^{2+}, some of the analyses would be classified as actinolite, based on Leake et al. (1997). This finding suggests that during routine semi-quantitative analyses of Vermiculite Mountain amphibole, as might be performed by an environmental asbestos analysis laboratory, the presence of actinolite might be reported. It is also possible that different laboratories could report the presence of different asbestos minerals from the same samples depending on the data reduction methods used.

Both SEM/EDS single-fiber and EPMA/WDS thin-section data occupy approximately the same compositional space, as shown in Figure 6. A few compositions that correspond to magnesioriebeckite and one to magnesio-arfvedsonite are indicated from the EPMA data. These amphibole types along with edenite (not identified in the EPMA data) were also found with SEM/EDS analyses. The magnesioriebeckite and magnesio-arfvedsonite EDS data points are all within 1σ error of richterite and/or winchite. The lack of statistically significant EDS data for magnesioriebeckite and magnesio-arfvedsonite suggests that these minerals may not exist in fibrous form. All of the EDS edenite analyses are within 2σ error of being classified as tremolite. All other minerals were identified in both thin sections and in the single fiber data. This comparison indicates that tremolite, winchite, and richterite (and possibly edenite) all occur

TABLE 2. -- *continued (2)*

Sample	16	20	25	25	25	10	12	14	16	24	30
Mineral	T	T	T	T	T	R	R	R	R	R	R
Wt% Oxides											
F	0.18	0.00	0.08	0.47	0.21	0.65	0.08	0.17	0.34	0.74	0.52
Na_2O	2.26	1.29	2.62	2.49	2.28	4.13	3.73	4.38	4.96	3.90	4.48
MgO	22.1	21.7	21.9	21.9	21.9	23.0	21.1	20.3	19.8	21.2	21.4
Al_2O_3	0.71	0.56	0.30	0.32	0.25	0.01	0.12	0.20	0.29	0.36	0.27
SiO_2	55.6	55.2	57.3	57.3	57.3	58.1	55.3	55.2	56.2	56.8	56.9
Cl	0.02	0.03	0.01	BDL	BDL	0.01	BDL	BDL	BDL	0.01	BDL
K_2O	0.86	0.58	0.78	0.75	0.68	1.56	0.77	1.06	0.97	1.20	1.22
CaO	10.1	10.70	10.2	10.3	10.5	7.79	7.45	6.11	5.76	8.03	7.43
TiO_2	0.11	0.10	0.01	0.04	0.06	0.20	0.21	0.12	0.04	0.07	0.16
MnO	0.07	0.10	0.10	0.10	0.10	0.09	0.05	0.09	0.08	0.13	0.12
FeO	2.40	4.00	3.73	3.82	3.52	2.35	5.61	6.56	7.49	5.08	5.08
O≡F,Cl	0.08	0.01	0.04	0.20	0.09	0.28	0.03	0.07	0.14	0.31	0.22
□TOTAL	94.32	94.24	96.96	97.21	96.63	97.59	94.33	94.13	95.73	97.25	97.34
Structural Formula											
Si	7.918	7.911	7.977	7.972	7.992	7.999	7.980	7.983	7.976	7.967	7.973
Al^{iv}	0.082	0.089	0.023	0.028	0.008	0.001	0.020	0.017	0.024	0.033	0.027
Sum T-site	8.000	8.000	8.000	8.000	8.000	8.000	8.000	8.000	8.000	8.000	8.000
Al^{iv}	0.037	0.006	0.026	0.025	0.034	0.001	0.001	0.017	0.024	0.026	0.016
Ti	0.012	0.011	0.001	0.004	0.006	0.021	0.022	0.013	0.004	0.007	0.017
Fe^{3+}	0.101	0.036	0.070	0.073	0.073	0.226	0.004	0.240	0.485	0.150	0.094
Mg	4.686	4.629	4.547	4.535	4.550	4.727	4.534	4.374	4.179	4.433	4.465
Fe^{2+}	0.163	0.318	0.355	0.363	0.337	0.026	0.438	0.355	0.307	0.383	0.407
Mn	0.000	0.000	0.000	0.000	0.000	0.000	0.000	0.000	0.000	0.000	0.000
Sum C-site	5.000	5.000	5.000	5.000	5.000	5.000	5.000	5.000	5.000	5.000	5.000
Mg	0.000	0.000	0.000	0.000	0.000	0.000	0.000	0.000	0.000	0.000	0.000
Fe^{2+}	0.021	0.126	0.008	0.009	0.001	0.019	0.234	0.198	0.097	0.062	0.094
Mn	0.008	0.012	0.012	0.012	0.012	0.010	0.006	0.010	0.009	0.015	0.014
Ca	1.542	1.643	1.520	1.537	1.562	1.150	1.151	0.946	0.875	1.206	1.115
Na	0.429	0.219	0.460	0.442	0.425	0.821	0.608	0.846	1.018	0.716	0.777
Sum B-site	2.000	2.000	2.000	2.000	2.000	2.000	2.000	2.000	2.000	2.000	2.000
Na	0.194	0.138	0.247	0.231	0.192	0.281	0.437	0.383	0.348	0.343	0.441
K	0.155	0.106	0.138	0.134	0.121	0.274	0.141	0.196	0.176	0.215	0.218
Sum A-site	0.350	0.244	0.385	0.364	0.313	0.554	0.578	0.579	0.524	0.558	0.659
Total Cations	15.350	15.244	15.385	15.364	15.313	15.554	15.578	15.579	15.524	15.558	15.659

continued next page

in fibrous or asbestiform habit in the Vermiculite Mountain rocks, and also that the EPMA data include the majority of the suite of amphibole compositions that are present in the deposit.

The EDS single-fiber data provide information on the distribution of compositions of the friable and fibrous amphiboles. These analyses are plotted for each sample in Figure 7. For many samples, the compositions cluster in relatively small regions of the diagram as compared to Figure 6. A few samples, such as 8, 16, and 23, show a wider range of compositions. Compositions of several of the samples (5, 7, 9, 13, 21, and 24) cluster entirely within the winchite region of the diagram. Several samples (1, 3, 6, 25, 28, and 29) have a significant amount of richterite, but no samples plot entirely within the richterite field. Samples 8, 20, and 23 show the highest concentrations of tremolite.

The classification of a small portion of the Vermiculite Mountain amphibole as edenite (samples 4, 8, and 19) by EDS remains uncertain. A natural occurrence of fibrous fluoroedenite from Sicily was reported by Gianfagna and Oberti (2001). It is likely, however, that in our analyses, microcrystalline calcite, intergrown with the amphibole, could be contributing Ca to the totals, thus increasing the amount of Na assigned to the A-site. Nevertheless, some of our SEM/EDS analyses calculate as edenite with no evidence of calcite. However, these analyses are within analytical error of tremolite and richterite.

Edenite usually contains Al in the T-site to balance Na in the A-site, which was not found in the Vermiculite Mountain amphibole. The classification scheme of Leake et al. (1997) is not clear with regard to calcic amphiboles of this composition, i.e., amphiboles containing more than 0.5 (Na + K) in the A-site, less than 0.5 Na in the B-site, and more than 7.5 Si in the T-site. Leake (1978) includes the term "silicic-edenite," which would cover the compositions found in the Vermiculite Mountain amphibole. This name was dropped in the subsequent and final classification system (Leake et al. 1997) and it appears that the intended name for amphiboles of this composition is edenite. Further investigations are underway regarding the presence of edenite.

Morphology

In general, the Vermiculite Mountain amphiboles have two types of occurrence: vein-fillings and replacement of the primary pyroxene of the Rainy Creek complex. The textures displayed by the amphibole and associated minerals are indicative of their hydrothermal origin. Traditionally, amphibole asbestos is thought to occur as a vein-filling mineral formed during

hydrothermal alteration in a tensional environment (Zoltai 1981) or as a low-temperature alteration product formed in a stress-free environment (Dorling and Zussman 1987). In a substantial portion of our samples, the amphiboles appear to be forming as direct replacements of pyroxene, probably by the infiltration of fluids in microfractures. Examples of these two modes of formation are shown in Figure 8. Figure 8a shows a cross-section of a vein filled with symmetrically matching layers of amphibole and other minerals including calcite, K-feldspar, titanite, and pyrite. The amphibole becomes finer-grained toward the vein center but the composition of the winchite amphibole remains fairly constant across the vein. Figure 8b shows a portion of a sample in which the primary pyroxene augite crystals are being replaced by fibrous amphibole winchite and richterite. Figure 8c shows a detailed view of this replacement within a single pyroxene crystal. The long axis of the fibrous amphibole is crystallo-graphically aligned with the original pyroxene crystal.

In portions of all of the samples studied, the amphibole is intergrown with accessory minerals such as calcite, K-feldspar, quartz, and titanite. The accessory minerals range in size from millimeters to sub-micrometer. Extremely fine-grained crystals of these minerals are commonly intergrown and often crystallographically oriented with the amphibole (Fig. 9). These minerals were found in thin section as well as in the SEM samples of friable dust, often in acicular form.

The Vermiculite Mountain amphiboles show a range of morphologies from prismatic to asbestiform (Fig. 10). Much of the fibrous amphibole seen in the SEM micrographs (Figs. 2 and 10) is composed of acicular and, some cases, needle-like particles. Splayed ends and curved fibers are present, but are not particularly common. Fibril diameter in the Vermiculite Mountain asbestiform amphibole ranges from approximately 0.1 to 1 μm. Individual fibrils less than 0.2 μm in diameter are rare, and fiber bundles are often composed of different-sized fibrils. Many of the characteristics generally associated with "commercial-grade" asbestos, such as curved fibers and bundles with splayed ends (Perkins and Harvey 1993) are present but are not common in the Vermiculite Mountain amphibole.[2] The material, however, is very friable and even gentle handling of what appears to be a solid, coherent rock can liberate very large numbers of extremely fine fibers as seen in SEM images (Figs. 2 and 10) and in size-distribution plots of material sampled from the inside of the sample bags (Fig. 11).

TABLE 2 --*continued* (3)

Sample	30	30	10	10	10	10	10	12	10
Mineral	R	R	MR	MR*	MR*	MR*	MR*	MR	MA
Wt% Oxides									
F	0.56	0.17	0.45	0.30	0.27	0.45	0.49	0.09	0.52
Na_2O	4.59	4.26	7.04	7.11	6.92	6.85	6.98	6.51	6.76
MgO	20.9	21.0	17.1	16.8	16.4	16.8	17.0	17.5	17.8
Al_2O_3	0.45	0.35	0.04	0.07	0.08	0.07	0.08	0.25	0.08
SiO_2	57.3	56.6	56.5	57.1	56.8	56.9	56.9	56.4	56.8
Cl	BDL	BDL	0.01	BDL	BDL	BDL	0.01	BDL	BDL
K_2O	1.29	1.32	1.09	0.95	0.96	0.98	0.97	0.81	1.06
CaO	7.31	7.26	2.03	2.07	1.92	2.32	2.07	2.20	2.70
TiO_2	0.05	0.04	0.47	0.15	0.39	0.44	0.41	0.58	0.25
MnO	0.12	0.06	0.07	0.09	0.05	0.09	0.08	0.04	0.04
FeO	5.29	5.22	11.5	12.3	12.3	11.4	11.3	11.0	11.0
O ≡ F,Cl	0.23	0.07	0.19	0.13	0.11	0.19	0.21	0.04	0.22
□TAL	97.65	96.16	96.15	96.76	96.06	96.13	96.03	95.39	96.89
Structural Formula									
Si	7.979	7.971	7.997	8.006	8.011	8.022	8.012	7.980	7.993
Al^{iv}	0.021	0.029	0.003	0.000	0.000	0.000	0.000	0.020	0.007
Sum T-site	8.000	8.000	8.000	8.006	8.011	8.022	8.012	8.000	8.000
Al^{vi}	0.053	0.029	0.004	0.012	0.013	0.011	0.013	0.020	0.007
Ti	0.005	0.004	0.049	0.016	0.042	0.046	0.043	0.062	0.026
Fe^{3+}	0.241	0.285	1.097	1.240	1.272	1.177	1.211	1.123	0.955
Mg	4.348	4.402	3.604	3.505	3.456	3.532	3.578	3.690	3.738
Fe^{2+}	0.354	0.280	0.246	0.200	0.182	0.164	0.115	0.105	0.274
Mn	0.000	0.000	0.000	0.011	0.006	0.011	0.009	0.000	0.000
Sum C-site	5.000	5.000	5.000	4.984	4.972	4.942	4.968	5.000	5.000
Mg	0.000	0.000	0.000	0.000	0.000	0.000	0.000	0.000	0.000
Fe^{2+}	0.021	0.050	0.023	0.000	0.000	0.000	0.000	0.074	0.067
Mn	0.014	0.007	0.009	0.000	0.000	0.000	0.000	0.005	0.005
Ca	1.091	1.096	0.307	0.310	0.290	0.350	0.313	0.333	0.407
Na	0.875	0.847	1.662	1.690	1.710	1.650	1.687	1.588	1.521
Sum B-site	2.000	2.000	2.000	2.000	2.000	2.000	2.000	2.000	2.000
Na	0.364	0.316	0.270	0.243	0.181	0.221	0.220	0.196	0.323
K	0.229	0.238	0.196	0.170	0.173	0.175	0.173	0.146	0.191
Sum A-site	0.593	0.554	0.466	0.414	0.354	0.396	0.393	0.341	0.513
Total Cations	15.593	15.554	15.466	15.403	15.336	15.360	15.373	15.341	15.513

* These analyses display T site totals slightly higher than what is recommended by Leake et al. (1997) for determination of percent Fe^{+3}, however, the T site error is well below 1% and Fe^{+3} values are in agreement with other analyses of similar composition.

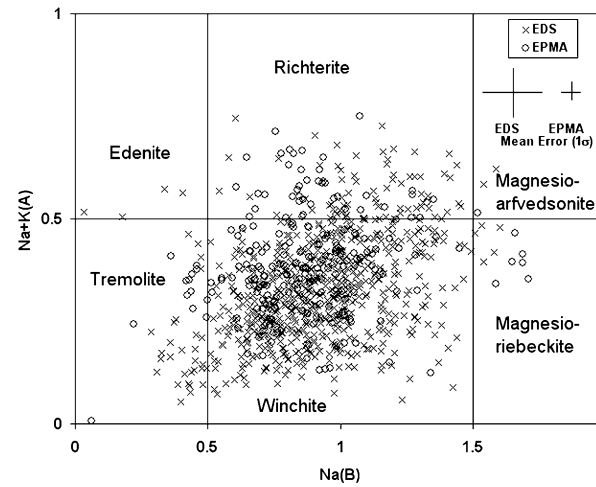

FIGURE 6. EPMA/WDS and SEM/EDS data showing the entire range of amphibole species found from all 30 samples. See text for details.

[2]The definition of asbestiform found in Perkins and Harvey (1993) is for optical identification of commercial-grade asbestos used in building materials.

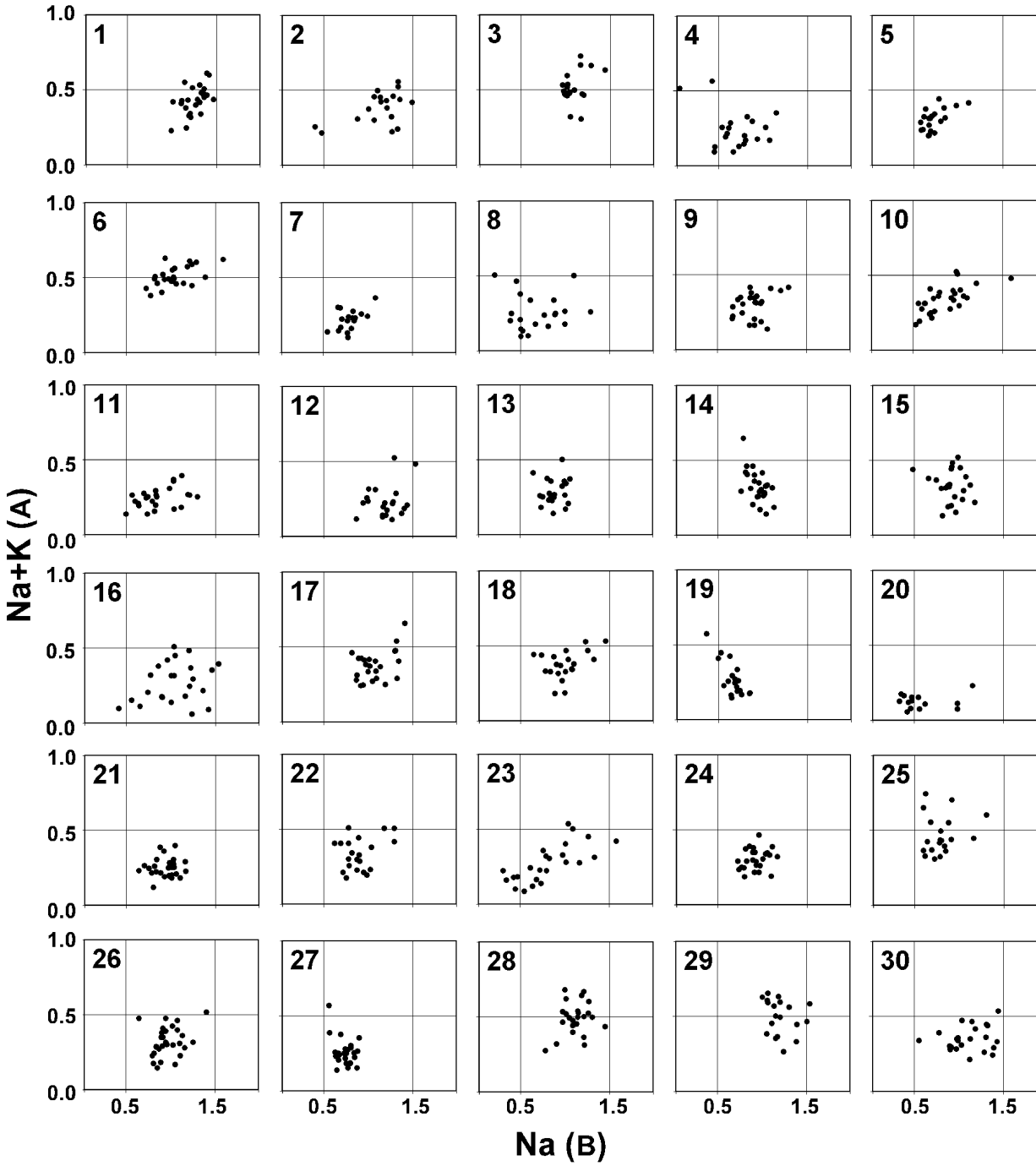

FIGURE 7. EDS data for 30 samples showing the distribution of compositions of the fibrous and friable amphibole for each sample location at the mine (see Fig. 1). Sample number is in the top left corner of each plot (see Fig. 1). Mineral fields are the same as shown in Figure 6.

The data shown in Figure 11 are plotted as diameter vs. length and diameter vs. aspect ratio, respectively. These data, which were obtained from samples 4, 10, 16, 20, and 30, represent the range of amphibole compositions sampled. For the most part, all of the samples produce fibers in a similar size range. It is important to remember that these samples were not ground to produce these particles. The fibers were collected on the SEM stubs by touching the stub to the inside of the original sample bag after it was received from the field and other sample material was removed. Approximately 40% of the particles are greater than 5 μm in length and have aspect ratios greater than 3. This finding means that, based on size, these particles are countable as asbestos by most approved methods such as Crane (1992). Even if more conservative counting criteria are employed, such as ≤0.5 μm diameter with aspect ratios of ≥10, approximately 30% of the particles would be included. These observations dem-

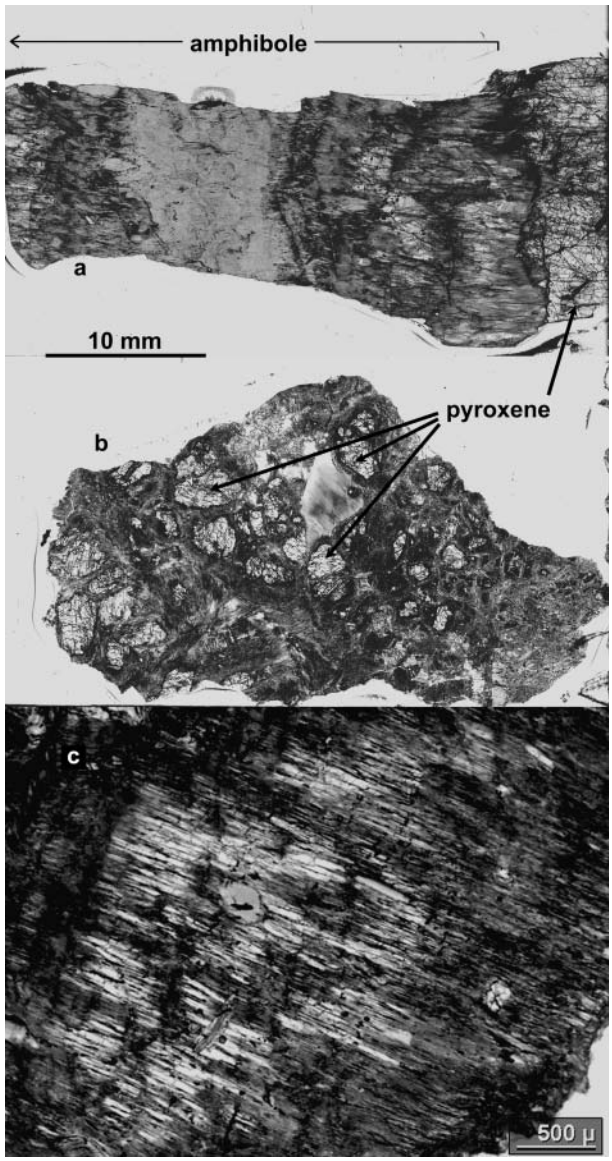

FIGURE 8. Transmitted-light images of entire polished thin sections showing: (**a**) amphibole filling a vein with symmetric dark and light (center of the vein) layers and (**b**) amphibole (dark areas) replacing pyroxene crystals. (**c**) A large single pyroxene crystal (bright areas) partly replaced by amphibole (dark areas) along crystallographically oriented planes is shown in transmitted, cross polarized light.

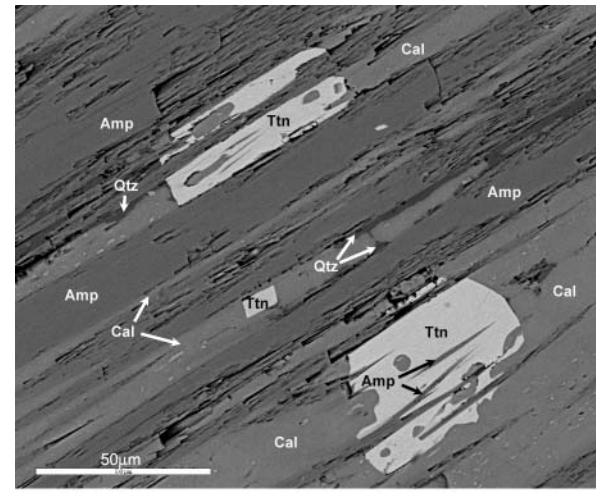

FIGURE 9. Back-scattered electron image of an area of a thin section of sample 24 showing massive and fibrous amphibole (Amp) intergrown with secondary calcite (Cal), titanite (Ttn), and quartz (Qtz). Note the fibrous amphibole enclosed by the large titanite grain at lower right, indicating order of crystallization.

onstrate that the Vermiculite Mountain amphiboles, with minimal disturbance, can easily degrade into highly acicular particles that are less than 3 µm in diameter and are therefore respirable (National Academy of Sciences 1984).

DISCUSSION

The amphibole samples analyzed in this study show a large range in chemical composition. This range is consistent with varying degrees of, and possibly different episodes of, alteration of the original pyroxenite body by hydrothermal fluids associated with the intrusion of syenite and related rocks. The variations in composition seen in the EDS data in Figure 7 do not appear to correlate directly with sample location. Samples 5, 6, and 7 were collected in close proximity to each other. Samples 5 and 7 show a similar compositional distribution, but the compositions in Sample 6 are distinctly different. Sample pairs 4 and 28, and 27 and 29 were collected from locations that are relatively close to each other and well within the biotite pyroxenite. Both of these show distinctly different amphibole compositions within each pair. These data suggest that the compositional differences are not due to location or gross zoning within the intrusion. The variations are more likely due to the reaction of pyroxene with different compositions of hydrothermal fluids associated with the quartz-rich veins and the trachyte, phonolite, and syenite dikes described by Boettcher (1966b, 1967). The variations also could be due to differences in the duration of fluid-rock interaction.

In addition to compositional variations among samples, EPMA data show compositional variations on the micrometer scale. Several samples showed changes in the amphibole mineral within single grains or fiber structures. Figure 12a shows a non-fibrous amphibole crystal with concentric zoning from magnesioriebeckite in the core to winchite at the rim. Figure 12b shows a single amphibole grain with compositions ranging from tremolite to winchite.

The variability of compositions on the micrometer scale can produce single fibrous particles that can have different amphibole names at different points of the particle. This type of variation has implications for the regulatory community. Morphologically, such structures might be considered fibers by most analytical protocols (Crane 1992, 1997; Baron 1994). However, by some current regulations and approved analytical methods, the variable chemistry of these particles could exclude them from being classified as "asbestos." This complexity creates a dilemma for the analyst who is charged with determining

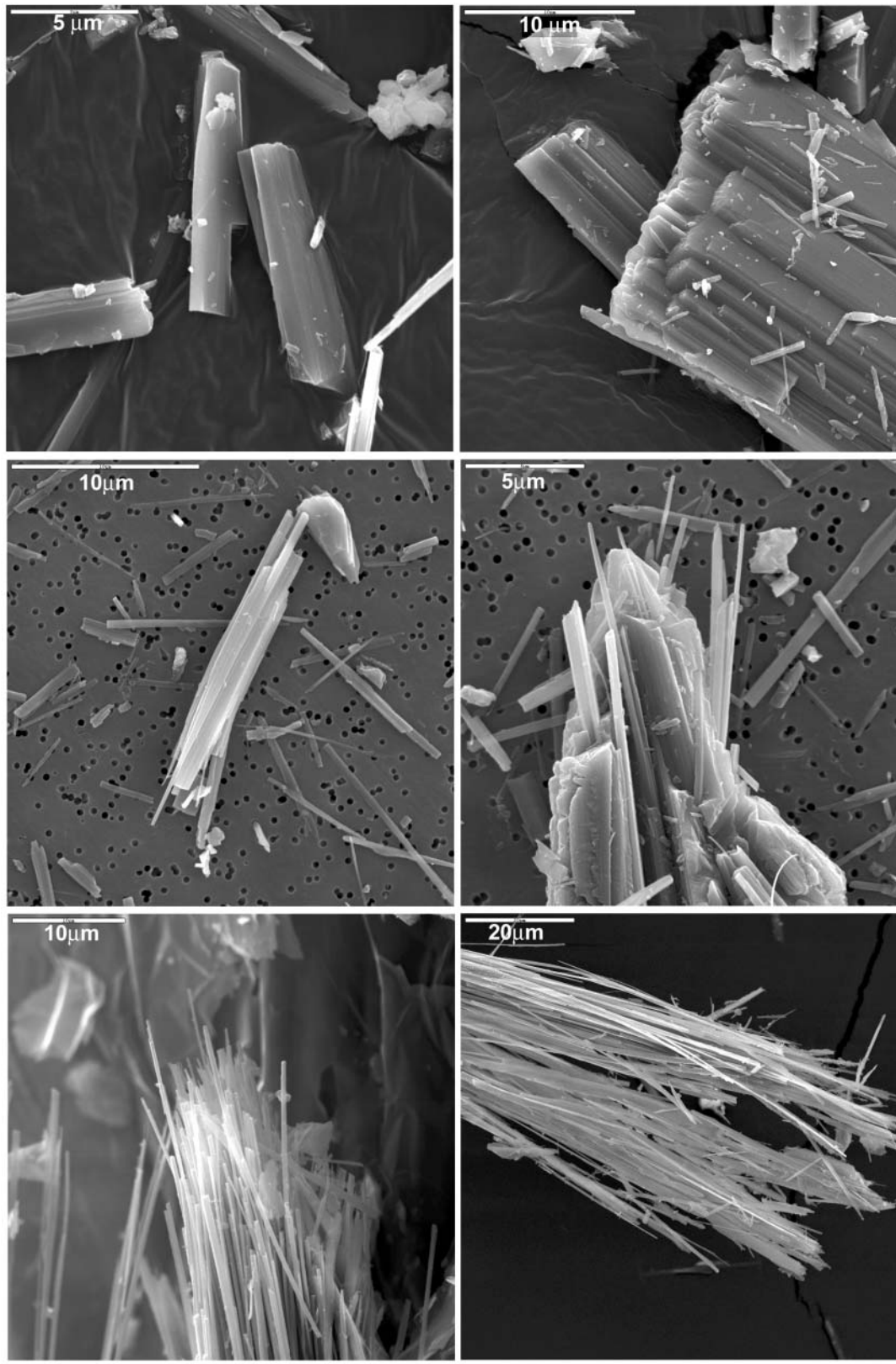

FIGURE 10. Electron micrographs of typical morphological types of Vermiculite Mountain amphiboles. The morphologies range from prismatic crystals (upper left) to long fibers and bundles (lower right).

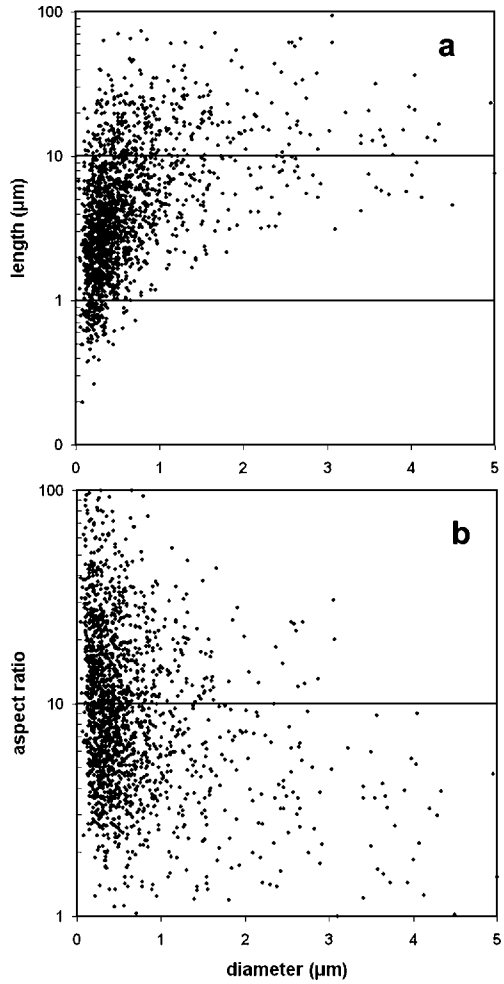

FIGURE 11. Amphibole particle size data from samples 4, 10, 16, 20, and 30 for particle diameters 5 µm and less, plotted as length vs. diameter (**a**) and aspect ratio (length:diameter) versus diameter (**b**).

whether asbestos is present in a sample and at what level.

A further dilemma arises from the fact that none of the present regulatory analytical methods (with the possible exception of well-calibrated SEM/EDS analysis using calibration standards similar to EPMA/WDS) can accurately differentiate the amphiboles present in the asbestiform materials from Vermiculite Mountain. Even with standard optical techniques, the results can be ambiguous (Wylie and Verkouteren 2000). This ambiguity arises because the mineralogical community currently classifies amphiboles on the basis of crystal chemistry, and high precision and accuracy in the microanalytical technique employed are required to classify an amphibole accurately. Analytical electron microscopy (TEM/EDS) provides compositional information, but the thickness of the sample must be known to provide accurate chemistry. This information is normally not available during routine TEM analysis of asbestos fibers as would be performed when following approved asbestos analysis methods such as ISO 10312 (1995).

The problem of classification is complicated further when the oxidation state of Fe is considered. This complication is illustrated in Figure 3, where the amphibole-species distribution is seen to shift significantly when the analyses are calculated using pure Fe^{+2} and Fe^{+3} end-members. The degree of accuracy and precision required to determine the correct oxidation state of Fe is not achievable during routine microanalysis of small, unpolished, single structures by SEM/EDS or TEM/EDS. Therefore, any regulatory distinction between minerals that requires knowledge of the oxidation state of Fe, such as the distinction between tremolite and actinolite, is technically not possible without a full quantitative chemical analysis.

Our analysis of unpolished, micrometer-sized particles of a basalt glass standard by SEM/EDS resulted in the 2σ errors as high as ±25% relative for Na and ±14% for Fe. Without the ability to correlate unpolished single-fiber SEM/EDS analyses with EPMA data from polished samples, it would be extremely difficult to confirm the presence of any of the amphibole min-

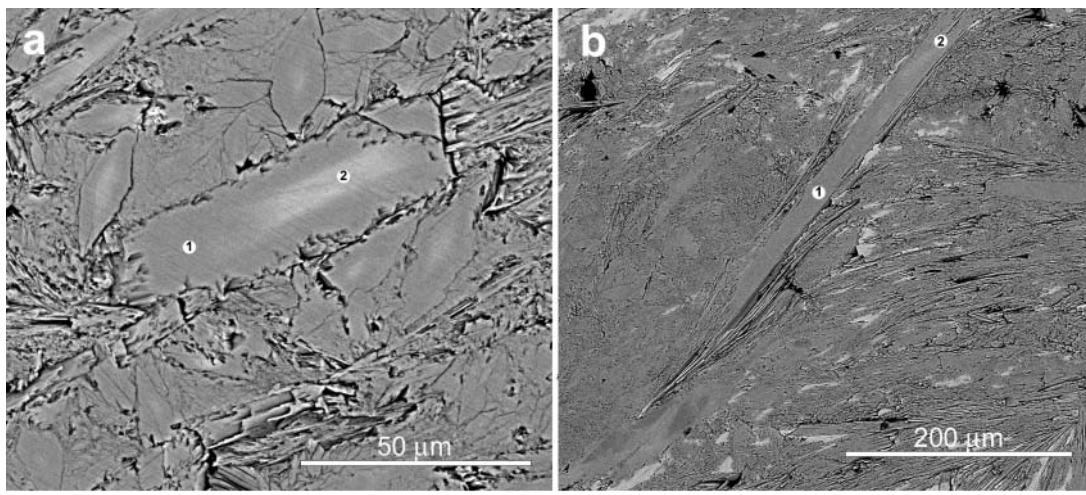

FIGURE 12. (**a**) Back-scattered electron image showing a prismatic amphibole grain with a rim of winchite (point 1) and a core of magnesioriebeckite (point 2), partially surrounded by fibrous amphibole. Other grains of similar composition can be seen above and below. (**b**) Backscattered electron image showing a large single amphibole structure (center) exhibiting fibrous habit at the ends and along the margins. Point 1 is tremolite and point 2 is winchite.

erals identified in this study by EDS alone. We therefore recommend that the International Mineralogical Association classification system (Leake et al. 1997) for amphiboles not be used for regulatory purposes in cases where high analytical precision and accuracy cannot be demonstrated.

If a microanalytical technique does not have the precision and accuracy to classify amphibole asbestos correctly according to current mineralogical criteria, then how should asbestos, such as that found at Vermiculite Mountain, be classified? Within much of the existing asbestos literature, mineral names are not applied in a uniform manner and are not all consistent with presently accepted mineralogical nomenclature and definitions. Tremolite and actinolite (members of the solid-solution series tremolite-ferroactinolite), and anthophyllite are mineral names recognized by the Subcommittee on Amphiboles of the International Mineralogical Association (Leake et al. 1997). For these three amphibole species, the term "asbestiform" usually must precede the mineral name, or the term asbestos must be added after the mineral name to denote a regulated material. The name amosite, derived from an acronym for Asbestos Mines of South Africa, is generally considered to refer to the asbestiform varieties of minerals in the cummingtonite-grunerite solid-solution series (Rabbitt 1948; Vermas 1952; Bowles 1959). Crocidolite is the asbestiform variety of the amphibole riebeckite. This inconsistency in the application of nomenclature can cause significant problems for asbestos analysts, medical professionals, and regulators who are unfamiliar with the principles of mineralogic classification, including solid-solution. In addition to the five amphibole asbestos "minerals" normally cited in the regulatory literature, many other amphibole minerals have been reported to occur in asbestiform and fibrous habit (Zoltai 1981; Wylie and Huggins 1980). A few methods and regulations (e.g., ISO 10312, method for TEM analysis of asbestos) recognize the possible existence of other asbestiform amphiboles, but make no attempt to identify or define them mineralogically.

To complicate further the problems in nomenclature cited above, the nuances of mineralogical classification systems are often not specified or are not well defined in the regulatory literature for many potentially fibrous and asbestiform amphiboles (Lowers and Meeker 2002). In many cases, nominal compositions are given for a mineral but no chemical boundaries are specified. Furthermore, the techniques and methods available and approved for the analysis and classification of asbestos by regulatory entities are often not capable of adequately identifying or distinguishing many of these minerals according to current mineralogical guidelines (such as Leake et al. 1997). This problem is particularly true for microanalytical techniques such as TEM and SEM employing qualitative or semiquantitative EDS.

By virtue of the age of regulatory documents, the current regulatory language (i.e., Bridbord 1976; OSHA 1992) omits richterite and winchite. A better alternative for regulatory nomenclature, consistent with modern mineralogical terminology and analytical capabilities, would be to replace the names of the five amphiboles, tremolite asbestos, actinolite asbestos, crocidolite, amosite, and anthophyllite asbestos by the term "asbestiform amphibole" as suggested by Wylie and Verkouteren (2000) or by "fibrous amphibole," if such a description is deemed necessary by the medical and health science community. Barring any such changes in the current regulatory language, the Vermiculite Mountain amphibole asbestos could, for the purposes of regulation only, be considered equivalent to tremolite or soda-tremolite asbestos in accordance with current and past industrial terminology for the Vermiculite Mountain amphiboles.

In addition to chemistry, morphology is a primary factor in evaluation of the asbestiform and fibrous amphiboles. Nomenclature is again a key issue in a discussion of morphological characteristics of amphiboles, particularly those from Vermiculite Mountain. Amphiboles can occur in fibrous and non-fibrous forms. Fibrous amphiboles can further be classified as asbestiform and non-asbestiform. The term asbestiform is usually applied to populations of single-crystal fibrils (the smallest structural unit of a fiber), which occur in bundles and possess certain characteristics including high aspect ratio, high tensile strength, and flexibility (Zoltai 1981; Perkins and Harvey 1993; Wylie 2000). Another class of amphibole particles, cleavage fragments, can exist in blocky or acicular habit. Regardless of aspect ratio, cleavage fragments are formed by the breaking of a larger crystal. Interestingly, Ahn and Bueck (1991) have described asbestiform riebeckite from Western Australia that appears to have formed by the separating or breaking of larger crystals on dislocation planes of weakness along (100) and (110). A similar formation mechanism was proposed by Veblen (1980) for a sample of asbestiform anthophyllite. These findings obscure somewhat the traditional definition of asbestiform. The Vermiculite Mountain amphiboles serve to underscore the fact that traditional morphological definitions of asbestos may not adequately define amphibole mineral fibers from a toxicological and regulatory perspective.

Within the asbestiform amphibole minerals median diameters vary. Veblen and Wylie (1993) presented data suggesting that tremolite asbestos and anthophyllite asbestos fibers have larger diameters (median about 0.45 μm), and riebeckite asbestos fibers have smaller diameters (median about 0.2 μm). Byssolite is a term that is sometimes applied to single acicular amphibole crystals with an average diameter of about 1–2 μm (Veblen and Wylie 1993) or "often wider than 1 μm" (Wylie 1979). Our data show the median diameter of the respirable fibrous component (less than 3 μm in diameter) of five Vermiculite Mountain amphibole samples to be 0.44 μm. The average diameter for the same set of particles is 0.56 ± 0.45 μm (1σ). From these data, the diameter of the Vermiculite Mountain amphiboles appears to be at the upper range for asbestos and overlaps with the size range cited for byssolite.

Cleavage fragments were specifically excluded from material regulated by OSHA in 1992 (OSHA 1992). Therefore, regardless of any mineralogical, physical, or toxicological differences that might exist among acicular cleavage fragments, byssolite, and asbestiform fibers, differentiation among these classes of particles has become an issue. With the amphiboles, the morphologic distinction between asbestiform fibers and cleavage fragments can be made readily in many cases. This distinction is particularly true when "high-grade" asbestos of commercial value is being compared to blocky cleavage frag-

ments generated by grinding an amphibole such as massive tremolite. The distinction is not as clear when non-commercial-grade fibrous amphiboles, like those from Vermiculite Mountain, are being evaluated. For example, by some definitions (e.g., Perkins and Harvey 1993; Wylie 2000), a population of "true" asbestos fibers should have a minimum mean aspect ratio of 20 for individual fibers longer than 5 μm. In our size analysis of five of the Vermiculite Mountain samples plotted in Figure 11, three samples had mean aspect ratios slightly higher than 20 whereas two had mean aspect ratios slightly lower. The mean aspect ratio for all five samples, for fibers longer than 5 μm, was only 22. The task of distinguishing between what traditionally has been considered asbestos from byssolite and cleavage fragments can become much more difficult if not impossible when only single amphibole particles are being evaluated, and a representative population of the amphibole material is not present. Such a situation can be encountered in the analysis of environmental samples of air, soil, or water.

The Vermiculite Mountain amphiboles display characteristics that include all of the above morphological classes in a continuum, from blocky crystals to acicular, non-flexible cleavage fragments, to extremely long flexible fiber bundles (Fig. 10). Most of the individual particles display features that are intermediate between cleavage fragments and long flexible fibers. There are no distinct morphological boundaries by which to categorize the amphiboles. In addition, the mineralogy of these amphiboles is not typical of most regulated asbestos. Given the variations and ambiguities in much of the morphological and mineralogical terminology expressed in the mineralogical, medical, industrial, and regulatory literature (Lowers and Meeker 2002), the Vermiculite Mountain amphiboles present a significant challenge to the analyst, to anyone attempting to classify the material with respect to existing definitions, and particularly to those attempting to extrapolate those morphological features and chemical compositions to potential toxicological properties.

ACKNOWLEDGMENTS

This paper has been greatly improved by review comments and suggestions from David Jenkins, Malcolm Ross, and Jill Pasteris. The authors thank Bradley VanGosen, Geoffrey Plumlee, and Douglas Stoeser for extremely helpful discussions and internal USGS review. We also thank Paul Lamothe and Monique Adams who contributed trace element analyses, and Roger Clark, Gregg Swayze, Chris Weis, Paul Peronard, Robert Horton, George Desborough, Raymond Kokaly, Joseph Taggart, Ben Leonard, and Mickey Gunter for their helpful discussions and input. This work was funded by the U.S. Geological Survey and the U.S. Environmental Protection Agency.

REFERENCES CITED

Ahn, J.H. and Bueck, P.R. (1991) Microstructures and fiber-formation mechanisms of crocidolite asbestos. American Mineralogist, 76, 1467–1478.

Baron, P.A. (1994) Asbestos by TEM, 4th ed. NIOSH Method 7402.

Bassett, W.A. (1959) The origin of the vermiculite deposit at Libby, Montana. American Mineralogist, 44, 282–299.

Boettcher, A.L. (1966a) Vermiculite, hydrobiotite, and biotite in the Rainy Creek Igneous complex near Libby, Montana. Clay Minerals, 6, 283–297.

———(1966b), The Rainy Creek igneous complex near Libby, Montana, 155 p. PhD thesis, The Pennsylvania State University, University Park.

———(1967) The Rainy Creek alkaline-ultramafic igneous complex near Libby, Montana, part I: Ultramafic rocks and fenite. Journal of Geology, 75, 526–553.

Bowles, O. (1959) Asbestos, a materials survey. U.S. Bureau of Mines Information Circular 7880, 94 p.

Bridbord, K. et al. (1976) Revised recommended asbestos standard. DHEW (NIOSH) Publication No. 77–169, 96 p.

Crane, D.T. (1992) Polarized light microscopy of asbestos. OSHA, Method No. ID-191, 20p; available on the worldwide web at http://www.osha.gov/dts/sltc/methods/inorganic/id191/id191.html

———(1997) Asbestos in air. OSHA, Method No. ID-160, 20p; available on the worldwide web at http://www.osha-slc.gov/dts/sltc/methods/inorganic/ id160/id160.html

Deer, W.A., Howie, R.A., and Zussman, J. (1963) Rock forming minerals, volume 2 chain silicates, 379 p. Longmans, Green and Co. Ltd, London.

Dorling, M. and Zussman, J. (1987) Characteristics of asbestiform and non-asbestiform calcic amphiboles. Lithos, 20, 469–489.

Gianfagna, A. and Oberti, R. (2001) Flouro-edenite from Biancavilla (Catania, Sicily, Italy): Crystal chemistry of a new amphibole end-member. American Mineralogist, 86, 1489–1493.

Gunter, M.E., Dyar D.M., Twamley B., Foit, F.F. Jr., and Cornelius, S. (2003) Composition, Fe^{3+}/Fe, and crystal structure of non-asbestiform and asbestiform amphiboles from Libby, Montana, U.S.A. American Mineralogist, This Volume.

ISO (1995) Ambient air determination of asbestos fibres, direct-transfer transmission electron microscopy method. ISO 10312:1995(E), 51p.

Kamp, D.W., Graceffa, P., Pryor, W.A., and Weitzman, S.A. (1992) The role of free radicals in asbestos-induced diseases. Free Radical Biology & Medicine, 12 293–315.

Langer, A.M., Nolan, R.P., and Addison, J. (1991) Distinguishing between amphibole asbestos fibers and elongate cleavage fragments of their non-asbestos analogues. In R.C. Brown et al. Eds., Mechanisms in Fibre Carcinogenesis, p. 253–267. Plenum Press, New York.

Larsen, E.S. (1942) Alkalic rocks of Iron Hill, Gunnison County, Colorado. U.S. Geological Survey Professional Paper 197-A, 64p.

Leake, B.E. (1978) Nomenclature of amphiboles. Mineralogical Magazine, 42, 533–563.

Leake, B.E., Woolley, A.R., Arps, C.E.S., Birch, W.D., Gilbert, M.C., Grice, J.D., Hawthorne, F.C., Kato, A., Kisch, H.J., Krivovichev, V.G., Linthout, K., Laird, J., Mandarino, J.A., Maresch, W.V., Nickel, E.H., Rock, N.M.S., Schumacher, J.C., Smith, D.C., Stephenson, N.C.N., Ungaretti, L., Whittaker, E.J.W., and Youzhi, G. (1997) Nomenclature of the amphiboles: Report of the subcommittee on amphiboles of the International Mineralogical Association, Commission on New Minerals and Mineral Names. American Mineralogist, 82, 1019–1037.

Lowers, H.A. and Meeker, G.P. (2002) Tabulation of asbestos-related terminology. U.S. Geological Survey Open-File Report 02-458; available on the worldwide web at http://pubs.usgs.gov/of/2002/ofr-02-458/index.html

Lybarger, J.A., Lewin, M., Peipins, L.A., Campolucci, S.S., Kess, S.E., Miller, A., Spence, M., Black, B., and Weis, C. (2001) Medical testing of individuals potentially exposed to asbestiform minerals associated with vermiculite in Libby, Montana, A report to the community [report dated August, 23, 2001]. Agency for Toxic Substances and Disease Registry; available on the worldwide web at http://www.atsdr.cdc.gov/asbestos/doc_phl_testreport.html

Meeker, G.P., Taggart, J.E., and Wilson, S.A. (1998) A basalt glass standard for multiple microanalytical techniques. Microscopy and Microanalysis, 4, 240–241.

Melzer, S., Gottschalk, M., Andrut, M., and Heinrich, M. (2000) Crystal chemistry of K-richterite-richterite-tremolite solid solutions: a SEM, EMP, XRD, HRTEM and IR study. European Journal of Mineralogy, 12, 273–291.

National Academy of Sciences (1984) Asbestiform fibers: nonoccupational health risks, p. 25–47. Committee on Nonoccupational Health Risks of Asbestiform Fibers, Board on Toxicology and Environmental Health Hazards, National Research Council. National Academy Press, Washington, D.C.

Nolan, R.P., Langer, A.M., Oechsle, G.E., Addison, J., and Colflesh, D.E. (1991) Association of tremolite habit with biological potential. In R.C. Brown, Ed., Mechanisms in Fibre Carcinogenesis, p. 231–251. Plenum Press, New York.

OSHA (1992) 29 CFR Parts 1910 and 1926 [Docket No. H-033-d], Occupational exposure to asbestos, tremolite, anthophyllite and actinolite. Federal Register, 57, 24310–24331; available on the worldwide web at http://www.osha.gov/pls/oshaweb/owasrch.search_form?p_doc_type=PREAMBLES&p_toc_level=1&p_keyvalue=Asbestos~(1992~-~Original)&p_text_version=FALSE

Pardee, J.T. and Larsen, E.S. (1928) Deposits of vermiculite and other minerals in the Rainy Creek District, near Libby, Mont. In Contributions to economic geology, U.S. Geological Survey Bulletin 805, 17–29.

Perkins, R.L. and Harvey, B.W. (1993) Test Method for the determination of asbestos in bulk building material. U.S. Environmental Protection Agency, EPA/600/r-93-116.

Popp, R.K. and Bryndzia, L.T. (1992) Statistical analysis of Fe^{3+}, Ti and OH in kaersutite from alkalic igneous rocks and mafic mantle xenoliths. American Mineralogist, 77, 1250–1257.

Rabbitt, J.C. (1948) A new study of the anthophyllite series. American Mineralogist, 33, 263–323.

Ross, M. (1981) The geologic occurrences and health hazards of amphibole and serpentine asbestos. In D.R. Veblen, Ed., Amphiboles and other hydrous pyriboles, p. 279–323. Reviews in Mineralogy, Mineralogical Society of America, Washington, D.C.

Small, J. and Armstrong, J.T. (2000) Improving the analytical accuracy in the analysis of particles by employing low voltage analysis. Microscopy and Microanalysis, 6, 924–925.

van Oss, C.J., Naim, J.O., Costanzo, P.M., Giese, R.F., Jr., Wu, W., and Sorling, A.F. (1999) Impact of different asbestos species and other mineral particles on pulmonary pathogenesis. Clay and Clay Minerals, 47, 697–707.

Veblen, D.R. (1980) Anthophyllite asbestos microstructures, intergrown silicates, and mechanisms of fiber formation. American Mineralogist, 65, 1275.

Veblen, D.R. and Wylie, A.G. (1993) Mineralogy of amphiboles and 1:1 layer silicates. In G.D. Gutheri, Jr. and B.T. Mossman, Eds., Health effects of mineral dusts, p.61–137. Reviews in Mineralogy, 28, Mineralogy Society of America, Washington, D.C.

Vermas, F.H.S. (1952) The amphibole asbestos of South Africa. Transactions and Proceedings of the Geological Society of South Africa, 55, 199–232.

Wylie, A.G. (1979) Optical properties of the fibrous amphiboles. Annals of the New York Academy of Sciences, 330, 611–619.

———(2000) The habit of asbestiform amphiboles-implications for the analysis of bulk samples. In M.E. Beard and H.L. Rooks, Eds., Advances in environmental measurement methods for asbestos. American Society for Testing of Materials Special Technical Publication 1342, 53–69.

Wylie, A.G. and Huggins, C.W. (1980) Characteristics of a potassian winchite-asbestos from the Allamoore talc-district, Texas. Canadian Mineralogist, 18, 101–107.

Wylie, A.G. and Verkouteren, J.R. (2000) Amphibole asbestos from Libby, Montana, aspects of nomenclature. American Mineralogist, 85, 1540–1542.

Zoltai, T. (1981) Amphibole asbestos mineralogy. In D.R. Veblen, Ed., Amphiboles and other hydrous pyriboles, p. 237–278. Reviews in Mineralogy, Mineralogical Society of America, Washington, D.C.

MANUSCRIPT RECEIVED MARCH 7, 2003
MANUSCRIPT ACCEPTED JULY 13, 2003
MANUSCRIPT HANDLED BY JILL PASTERIS